

# Fe<sub>3</sub>Si formation in Fe–Si diffusion couples

Y. ZHANG, D. G. IVEY

*Department of Chemical and Materials Engineering, University of Alberta,  
Edmonton, Alberta, Canada T6G 2G6  
E-mail: doug.ivey@ualberta.ca*

Two different types of bulk diffusion couples for the Fe–Si system, i.e. Fe/Si and Fe/Fe<sub>3</sub>Si, have been studied, with emphasis placed on the formation and growth of Fe<sub>3</sub>Si. Results indicate that Fe<sub>3</sub>Si forms initially in Fe/Si couples, followed by FeSi and then FeSi<sub>2</sub>. Fe<sub>3</sub>Si has a wide range of stoichiometry, from 10–25 at % Si; however, only stoichiometric Fe<sub>3</sub>Si appeared in Fe<sub>3</sub>Si diffusion layers of Fe/Si couples. Off-stoichiometric Fe<sub>3</sub>Si formed in Fe<sub>3</sub>Si/Fe couples. The free energy of Fe<sub>3</sub>Si and Fe–Si affinity are used to explain Fe<sub>3</sub>Si formation behaviour and the atomic diffusion mechanism in the Fe<sub>3</sub>Si lattice. © 1998 Kluwer Academic Publishers

## 1. Introduction

Recent work by one of the authors on bulk Fe–Si diffusion couples indicated that Fe<sub>3</sub>Si, which forms between  $\alpha$ -Fe and FeSi, is stoichiometric with a very narrow composition range [1]. This result appears to contradict the accepted version of the Fe–Si phase diagram (Fig. 1 [2]). Fe<sub>3</sub>Si, according to the diagram, has a wide range of stoichiometry, i.e. 10–25 at % Si. In this paper, we examine this question more carefully and propose an explanation for this apparent discrepancy.

Stoichiometric Fe<sub>3</sub>Si (Fe<sub>75</sub>Si<sub>25</sub>) has a DO<sub>3</sub> structure, i.e. a cubic superstructure consisting of four interpenetrating fcc sublattices, labelled A, B, C and D, with origins at the points (0, 0, 0) (1/4, 1/4, 1/4), (1/2, 1/2, 1/2) and (3/4, 3/4, 3/4) arranged regularly along the body diagonal (Fig. 2 [3]). Each A atom is at the centre of a cube with four B and four D atoms at the corners in tetrahedral arrangements. Similarly, each B atom is at the centre of a cube with four A and four C atoms at corners in cubic arrangements. In stoichiometric Fe<sub>3</sub>Si, iron atoms occupy the A, C and B sites. Thus, the iron atoms on equivalent (both structurally and magnetically) A and C sites have tetrahedral point symmetry with four iron [B] and four silicon [D] atoms as nearest neighbours. The Fe[B] atoms have cubic point symmetry with eight Fe[A,C] atoms as nearest neighbours, as in elemental bcc iron. Table I illustrates the neighbour configurations of stoichiometric Fe<sub>3</sub>Si [4].

For silicon compositions between 10 and 25 at %, off-stoichiometric Fe<sub>3</sub>Si forms DO<sub>3</sub>-related structures. Fe[A,C] sites can have either five iron and three silicon atoms as nearest neighbours or six iron and two silicon atoms as nearest neighbours [5]. The disordered, but DO<sub>3</sub>-related, Fe–Si alloys of this type are labelled as Fe<sub>3+y</sub>Si<sub>1-y</sub>, and they exist in the composition range  $0.4 \leq y \leq 1.0$  [3].

Paoletti and Passari [6] established that the magnetic moments of the two types of iron atoms were different; values of  $2.4\mu_B$  and  $1.2\mu_B$  ( $\mu_B$  is the Bohr magneton) were reported for Fe[B] and Fe[A,C] atoms, respectively. More recent data [3] suggest values of  $2.2$ – $2.4\mu_B$  and  $1.1$ – $1.35\mu_B$  for Fe[B] and Fe[A,C]. Swintendick [5] was the first to show that energy-band calculations, based on a rigid-level spin-polarized model, were capable of explaining the different magnetic moments on A, C and B sites.

Preferential site occupancy by transition metal impurities substituted into Fe<sub>3</sub>Si has been reported by several researchers [4, 7–9]. Impurities to the left of iron in the Periodic Table prefer Fe[B] sites and those beneath and to the right of iron enter Fe[A,C] sites.

Taking into account chemical and magnetic interaction, numerical values of energy parameters for the Fe–Si system have been determined using the Bragg–Williams–Gorsky (BWG) model and  $C_p$  (heat capacity) integration method [10–14]. The free energy of Fe<sub>3</sub>Si was found to decrease with decreasing iron concentration at a fixed temperature. In addition, Fe–Si affinity was found to be higher than Fe–Fe affinity [15, 16].

In the present work, two types of Fe–Si diffusion couples, i.e. Fe–Si and Fe–Fe<sub>3</sub>Si, are studied. The results obtained are discussed from the point of view of the free energy of Fe<sub>3</sub>Si, Fe–Si affinity, Fe<sub>3</sub>Si formation and atomic diffusion mechanisms in the Fe<sub>3</sub>Si lattice.

## 2. Experimental procedure

Diffusion couples were constructed from three different components: iron (99.95%), high-purity  $\langle 111 \rangle$  oriented single-crystal silicon and an Fe–Si alloy. The Fe–Si alloy, containing 25 at % Si, was produced in an induction furnace under an inert atmosphere (10% Ar

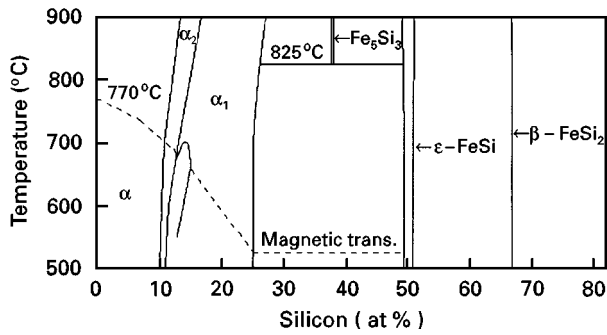


Figure 1 Fe-Si binary phase diagram.

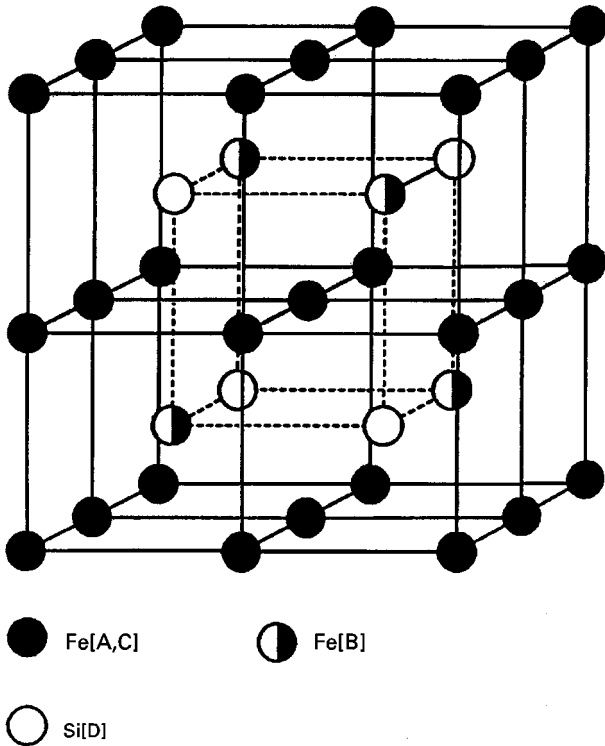


Figure 2 Schematic drawing of the  $\text{Fe}_3\text{Si}$  structure, showing the four different sites [3].

TABLE I Neighbour configuration in stoichiometric  $\text{Fe}_3\text{Si}$  [4]

Neighbour	1	2	3	4	5	6
$R^a$	0.43	0.5	0.705	0.83	0.86	1.00
A, C	4B 4D	6A, C	12A, C	12B 12D	8 A, C	6 A, C
B	8 A, C	6D	12B	24A, C	8D	6B
D	8 A, C	6B	12D	24A, C	8B	6D

<sup>a</sup>  $R$  is the distance expressed as a fraction of the lattice parameter  $a$ .

and 90% He). After the alloy was made, a homogenization anneal was done at  $1000^\circ\text{C}$  for 24 h. The diffusion couple assembly procedure has been given in detail elsewhere [1]; only a brief description will be given here. The surfaces of the iron, silicon and Fe-Si alloy were cut, ground and polished to thicknesses of 4.5, 3.0 and 4.5 mm, respectively; The faces of the pieces, that were to be in contact, were polished to a mirror finish on a  $6\ \mu\text{m}$  diamond wheel followed by

polishing on a  $0.05\ \mu\text{m}$   $\text{Al}_2\text{O}_3$  wheel. Polishing was done shortly before fabrication of the couples, in order to minimize oxidation of the polished surfaces. The couples were clamped together, sealed individually in quartz tubes with  $\sim 1\ \text{g}$  zirconium powder and annealed at  $700^\circ\text{C}$  for times ranging from 7–1000 h. After heat treatment, the couples were sectioned perpendicular to the contact plane and examined by optical and scanning electron microscopy (SEM). Energy dispersive X-ray (EDX) spectroscopy was used to determine the composition and composition profiles. FeSi was used as a standard for quantitative EDX.

### 3. Results

#### 3.1. Fe-Si couples

An SEM backscattered electron image for an Fe-Si couple annealed at  $700^\circ\text{C}$  for the shortest time studied (7 h) is shown in Fig. 3a. A corresponding composition profile is shown in Fig. 3b. This condition clearly represents the early stages of silicide formation and demonstrates that  $\text{Fe}_3\text{Si}$  forms initially in bulk couples. No FeSi or  $\text{FeSi}_2$ , the other two phases that would be expected to form at this temperature, were detected, at least within the resolution of the SEM.  $\text{Fe}_3\text{Si}$  was found to be stoichiometric, which is in agreement with previous work [1], with a composition corresponding to  $27 \pm 0.5\ \text{at}\ \%\ \text{Si}$ , which is

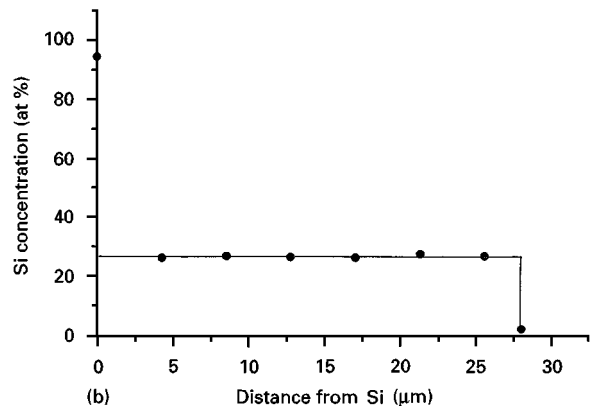
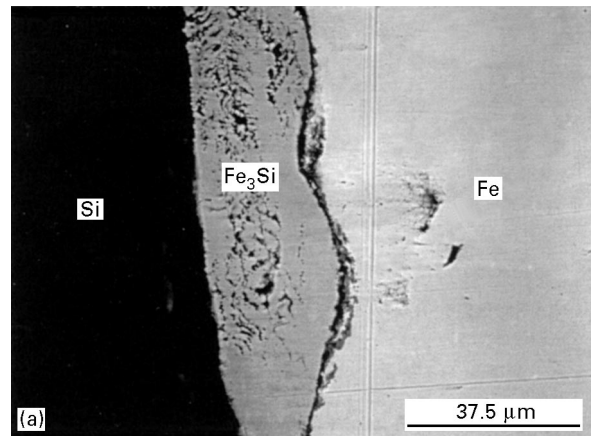


Figure 3 (a) SEM backscattered electron image of the diffusion zone of an Fe-Si couple annealed at  $700^\circ\text{C}$  for 7 h. (b) Concentration profile for the couple in (a).

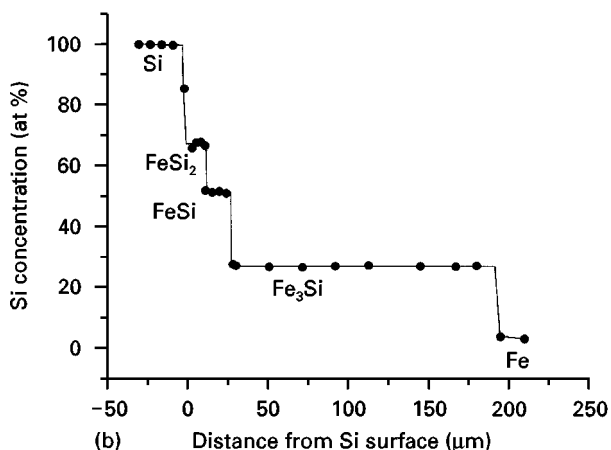
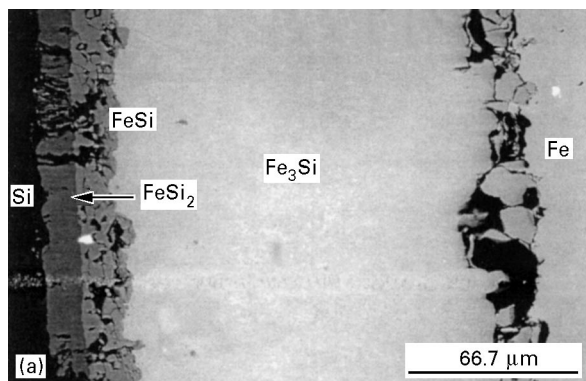


Figure 4 (a) SEM backscattered electron image of the diffusion zone of an Fe–Si couple annealed at 700 °C for 1007 h. (b) Concentration profile for the couple in (a).

slightly above the ideal value of 25 at % Si. The slightly higher silicon concentration, relative to the stoichiometric value, can be attributed to the fact that FeSi, and not Fe<sub>3</sub>Si, was used as the standard for EDX analysis. In any case, it is clear that the composition of Fe<sub>3</sub>Si is constant throughout the layer.

An SEM image and a concentration profile of an Fe–Si couple, annealed at 700 °C for 1007 h (longest annealing time), are shown in Fig. 4. Three silicide layers, corresponding to Fe<sub>3</sub>Si, FeSi and FeSi<sub>2</sub>, appear. FeSi was first observed to appear at ~23 h at 700 °C, while FeSi<sub>2</sub> was initially detected after 234 h. In both cases, the phases probably occurred sooner during annealing; however, the order of formation was Fe<sub>3</sub>Si, FeSi and then FeSi<sub>2</sub>. As observed for the lowest annealing time, the silicon concentration is constant within the Fe<sub>3</sub>Si layer. At the Fe<sub>3</sub>Si/ $\alpha$ -Fe interface, there are some cracks and missing material. This is because Fe<sub>3</sub>Si is brittle and is unable to deform during polishing like the  $\alpha$ -Fe adjacent to it.

EDX results from all Fe–Si diffusion couples studied showed only stoichiometric Fe<sub>3</sub>Si adjacent to  $\alpha$ -Fe. More than 100 positions along the Fe<sub>3</sub>Si/ $\alpha$ -Fe interface of each couple were examined in order to confirm this result.

Fe<sub>3</sub>Si growth was monitored to determine whether Fe<sub>3</sub>Si grew continually throughout the annealing process. The thickness of the Fe<sub>3</sub>Si layer is plotted as a function of the square root of annealing time in Fig. 5. It is clear that Fe<sub>3</sub>Si continues to grow throughout

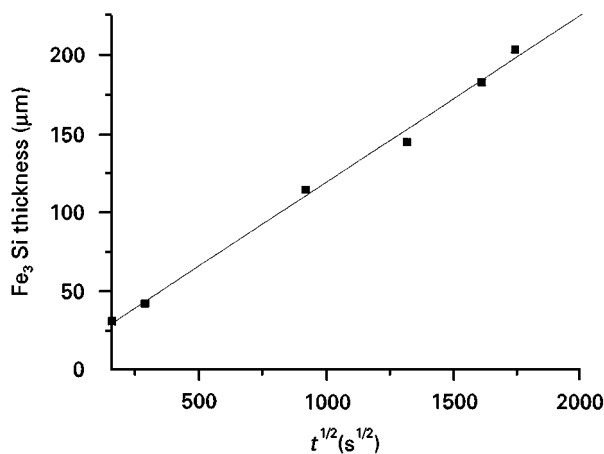


Figure 5 Plot of Fe<sub>3</sub>Si layer thickness versus time for Fe–Si couples annealed at 700 °C.

annealing and the linear dependence indicates that growth is diffusion controlled.

One possible explanation for the lack of off-stoichiometric Fe<sub>3</sub>Si is that the Fe<sub>3</sub>Si/ $\alpha$ -Fe interface region had separated during annealing, cutting off the supply of iron. If this was indeed the case, Fe<sub>3</sub>Si would convert to the most silicon-rich composition, i.e. stoichiometric Fe<sub>3</sub>Si. We believe that this is not the reason for the observed phenomenon, as crack-free regions along the interface were observed and these contained only the stoichiometric form of Fe<sub>3</sub>Si.

### 3.2. Fe<sub>3</sub>Si–Fe couples

A scanning electron micrograph and a corresponding concentration profile of the diffusion zone between Fe<sub>3</sub>Si and  $\alpha$ -Fe, for a couple annealed at 700 °C for 120 h, are shown in Fig. 6. A variable composition layer, identified as off-stoichiometric Fe<sub>3</sub>Si (Fig. 6a), is present at the Fe<sub>3</sub>Si/ $\alpha$ -Fe interface. The layer thickness (~15–20  $\mu$ m) was of the same order as the Fe<sub>3</sub>Si thickness in the Fe/Si couples annealed at 700 °C for only 7 h. Other couples produced similar results, i.e. off-stoichiometric Fe<sub>3</sub>Si formed between Fe<sub>3</sub>Si and Fe, and the Fe<sub>3</sub>Si growth rate was considerably lower compared with stoichiometric Fe<sub>3</sub>Si growth in Fe–Si couples.

## 4. Discussion

According to the accepted version of the Fe–Si phase diagram (Fig. 1), Fe<sub>3</sub>Si exists over a wide composition range (11–25 at % Si) at 600–700 °C. A concentration profile, then, from an Fe–Si diffusion couple annealed in this temperature range, should show a smooth transition from  $\alpha$ -Fe to Fe<sub>3</sub>Si. Composition profiles obtained here, and from a previous study [1], from Fe–Si couples indicate that only stoichiometric Fe<sub>3</sub>Si, and not Fe<sub>3+y</sub>Si<sub>1-y</sub>, forms. The concentration profiles (Figs 3b and 4b) have a vertical segment between stoichiometric Fe<sub>3</sub>Si and  $\alpha$ -Fe. On the other hand, off-stoichiometric Fe<sub>3</sub>Si does form in Fe–Fe<sub>3</sub>Si diffusion couples. The reason for this behaviour will be discussed below.

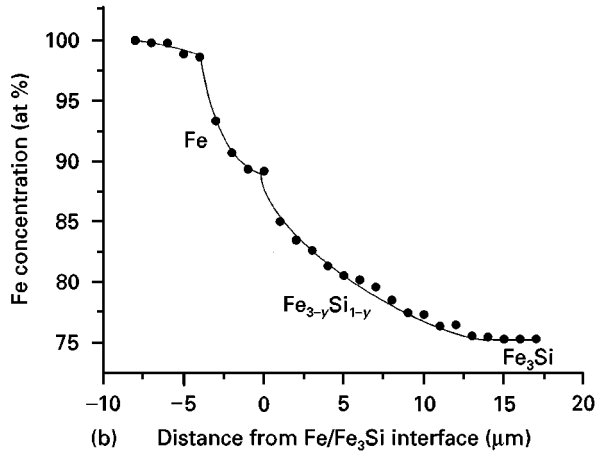
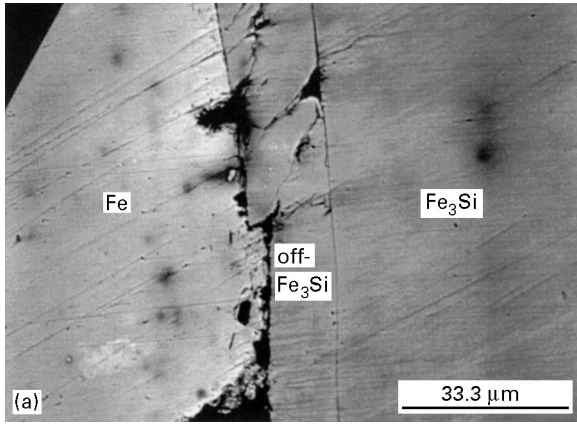


Figure 6 (a) SEM backscattered electron image of the diffusion zone of an Fe<sub>3</sub>Si–Fe couple annealed at 700 °C for 120 h. (b) Concentration profile for the couple in (a).

In a phase transformation, in general, there are two main factors controlling phase formation, i.e. thermodynamics (free energy change) and kinetics. Free energy calculations can be done, taking into account chemical and magnetic interactions, using a BWG model [10–14]. Calculations are briefly outlined below.

The most stable configuration corresponds to the minimum value in the configurational free energy,  $F_k$

$$F_k = U_k - TS_k \quad (1)$$

$U_k$  is the internal energy and can be expressed as

$$\begin{aligned} U_k = & U_k^0 - N\{4[W + J(2q - 1)^2]x^2 \\ & - 3wx^2 + 3/2w(y^2 + z^2)\} \\ & - NC_{Fe}C_{Si}\{4[W + J(2q - 1)^2] + 3w\} \\ & + 4NC_{Fe}J(2q - 1)^2 \end{aligned} \quad (2)$$

where

$$\begin{aligned} U_k^0 = & N\{4(C_{Fe}V_{FeFe} + C_{Si}V_{SiSi}) \\ & + 3(C_{Fe}v_{FeFe} + C_{Si}v_{SiSi})\} \end{aligned} \quad (3)$$

$S_k$  is the entropy term and has two components.

$$S_k = S_k^c + S_k^q \quad (4)$$

The chemical term is given as

$$S_k^c = -kN/4 \sum (p_{Fe}^L \ln p_{Fe}^L + p_{Si}^L \ln p_{Si}^L) \quad (5)$$

and the magnetic term is

$$S_k^q = -kNC_{Fe}[q \ln q + (1 - q) \ln(1 - q)] \quad (6)$$

$k$  is the Boltzman constant, while  $W$  and  $w$  are the chemical interchange energies for the process for nearest neighbours and next nearest neighbours, respectively.

$$W = -2V_{FeSi} + V_{FeFe} + V_{SiSi} \quad (7)$$

$$w = -2v_{FeSi} + v_{FeFe} + v_{SiSi} \quad (8)$$

$J$  is the magnetic interchange energy and  $N$  is the number of lattice sites. The chemical order parameters ( $x$ ,  $y$  and  $z$ ) are defined by the occupation probabilities,  $p_{Fe}^L$ , of iron in the four sublattices ( $L = A, B, C$  or  $D$ ).

$$x = 1/4(p_{Fe}^A + p_{Fe}^C - p_{Fe}^B - p_{Fe}^D) \quad (9)$$

$$y = 1/2(p_{Fe}^B - p_{Fe}^D) \quad (10)$$

$$z = 1/2(p_{Fe}^A - p_{Fe}^C) \quad (11)$$

$$p_{Fe}^A = C_{Fe} + x + z \quad (12)$$

$$p_{Fe}^C = C_{Fe} + x - z \quad (13)$$

$$p_{Fe}^B = C_{Fe} - x + y \quad (14)$$

$$p_{Fe}^D = C_{Fe} - x - y \quad (15)$$

$$p_{Si}^L = 1 - p_{Fe}^L (L = A, B, C, D) \quad (16)$$

$C_{Fe} = (1 - C_{Si})$  is the atomic concentration of iron. The magnetic order parameter is defined by spin state:  $0.5 < q < 1$ .

Free energy calculations for Fe<sub>3</sub>Si as a function of silicon atom fraction are shown in Fig. 7 for a temperature of 700 °C. The free energy decreases with increasing silicon fraction from 0.12 to 0.25 (12–25 at % Si). Thermodynamically, then, stoichiometric Fe<sub>3</sub>Si is the most stable form of Fe<sub>3</sub>Si, and would be expected to form preferentially to off-stoichiometric Fe<sub>3</sub>Si.

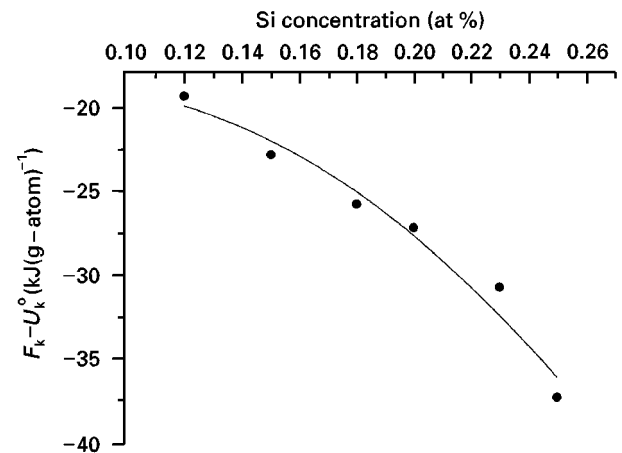


Figure 7 Plot of the difference between the configurational free energy term  $F_k$  and the internal energy term  $U_k^0$ , which is not a function of the order parameter, versus silicon atom fraction at 700 °C.

Reaction kinetics in diffusion couples are influenced by diffusional processes. Wever and Frohberg [16] and Bakker and Westerveld [17] have proposed that during diffusion in ordered  $\text{DO}_3$  lattices, the dominant species (iron in this case) jumps between the three iron sublattices only, i.e. A, C and B sublattices. This model has been confirmed by Sepiol and Vogl [18] using quasielastic Mössbauer spectroscopy (QMS) and quasielastic incoherent neutron scattering (QNS). Strong affinity exists between neighbouring iron and silicon atoms in  $\text{Fe}_3\text{Si}$ , which has been confirmed by Mössbauer spectroscopy [14]. It was found that silicon atoms share their 3s and 3p electrons with neighbouring iron atoms, thus filling the 3d states of the iron atoms. Garba and Jacobs [15] also calculated the affinity of  $\text{Fe}_3\text{Si}$ , using a tight binding model, and showed that a stronger affinity exists between neighbouring iron and silicon atoms than between neighbouring iron and iron atoms. Therefore, it is easier for iron to occupy iron sites than silicon sites, when iron atoms are diffusing in  $\text{Fe}_3\text{Si}$ . If iron atoms only diffuse via A, C and B sites in stoichiometric  $\text{Fe}_3\text{Si}$ , the system structure and free energy will be unchanged.

In off-stoichiometric  $\text{Fe}_3\text{Si}$ , a fraction of the iron atoms must occupy antisite positions on the D sublattice [18,19]. The antistructure has a slightly lower density and a slightly higher vacancy concentration than the ordered structure [17, 20]. Therefore, one might intuitively expect the antistructure to exhibit faster diffusion rates due to the higher vacancy concentration. Kikuchi and Sato [21], however, have shown that in an antisite disordered structure, an atom that has jumped to the “wrong” sublattice does not return immediately to a “correct” position, thereby inhibiting migration over long distances. As the iron concentration increases in  $\text{Fe}_3\text{Si}$ , the number of antisite positions increases which leads to a reduction in the diffusion coefficient. Diffusivities have been measured for stoichiometric and off-stoichiometric  $\text{Fe}_3\text{Si}$  [18]. At 720 °C, the diffusivity for  $\text{Fe}_{80}\text{Si}_{20}$  is a factor of five to ten times lower than that for stoichiometric  $\text{Fe}_3\text{Si}$ .

One can conclude from the above arguments that not only is stoichiometric  $\text{Fe}_3\text{Si}$  thermodynamically the most stable form of  $\text{Fe}_3\text{Si}$ , but its growth is also kinetically preferred over off-stoichiometric  $\text{Fe}_3\text{Si}$ . As such, only stoichiometric  $\text{Fe}_3\text{Si}$  would be expected in Fe/Si couples. In the Fe/ $\text{Fe}_3\text{Si}$  couples, off-stoichiometric  $\text{Fe}_3\text{Si}$  forms at the interface, but grows more slowly as a result of slower diffusion rates through the antistructure.

## 5. Conclusions

1. In the  $\text{Fe}_3\text{Si}$  diffusion layer of Fe–Si diffusion couples, only stoichiometric  $\text{Fe}_3\text{Si}$  forms. Off-stoichiometric  $\text{Fe}_3\text{Si}$  forms in  $\text{Fe}_3\text{Si}$ –Fe couples. These results are explained based on thermodynamic and kinetic arguments.

2. The thickness of the  $\text{Fe}_3\text{Si}$  layer in Fe–Si diffusion couples increases linearly as a function of the square root of the diffusion time.

3. At 700 °C stoichiometric  $\text{Fe}_3\text{Si}$  is the most stable form of  $\text{Fe}_3\text{Si}$ .

## Acknowledgement

This work was funded by a grant from the Natural Sciences and Engineering Research Council (NSERC) of Canada.

## References

1. N. R. BALDWIN and D. G. IVEY, *J. Phase Equilib.* **16** (1995) 1.
2. O. KUBASCHEWSKI, “Iron-Binary Phase Diagrams” (Springer, New York, 1982) p. 136.
3. J. KUDRNOVSKY, N. E. CHRISTENSEN and O. K. ANDERSEN, *Phys. Rev. B* (7) **43** (1993) 5924.
4. J. L. BUDNICK, T. ZHENGQUAN and D. M. PEASE, *Physica B* **158** (1989) 31.
5. A. C. SWINTENDICK, *Solid State Commun.* **19** (1976) 511.
6. A. PAOLETTI and L. PASSARI, *Nuovo Cim.* **XXXII** (1964) 1449.
7. T. J. BURCH, T. LITRENTA and J. I. BUDENICK, *Phys. Rev. Lett.* **33** (1974) 421.
8. C. BLAAUW, G. R. MACKAY and W. LEIPER, *Solid State Commun.* **18** (1975) 729.
9. S. PICKART, T. LITRENTA, T. J. BURCH and J. I. BUDINICK, *Phys. Lett. A* **53** (1975) 321.
10. G. INDEN and W. PITSCH, *Z. Metallkde* **62** (1971) 627.
11. G. SCHLATTE, G. INDEN and W. PITSCH, *ibid.* **65** (1974) 94.
12. G. INDEN and W. PITSCH, *ibid.* **63** (1972) 253.
13. G. INDEN, *ibid.* **68** (1977) 529.
14. M. B. STEARNS, *Phys. Rev.* **147** (1966) 439.
15. E. J. D. GARBA and R. L. JACOBS, *Phys. F Met. Phys.* **16** (1986) 1485.
16. H. WEVER and G. FROHBERG, *Z. Metallkde* **65** (1974) 747.
17. H. BAKKER and J. P. A. WESTERVELD, *Phys. Status Solidi b* **145** (1988) 409.
18. B. SEPIOL and G. VOGL, *Phys. Rev. Lett.* **71** (1993) 731.
19. K. SZYMAŃSKI, L. DOBRZYŃOKI and R. BURZYŃSKA, *Hyperf. Interact.* **59** (1990) 477.
20. K. SZYMAŃSKI, S. LEFEBVRE and M. BESSIERE, *Mater. Sci. Forum* **166–169** (1994) 433.
21. R. KIKUCHI and H. SATO, *Phys. Rev. B* **28** (1983) 648.

Received 24 December 1996  
and accepted 18 March 1998